Electronic Supplementary Material (ESI) for Nanoscale.
This journal is © The Royal Society of Chemistry 2016

Electronic Supplementary Information

Fabrication and bioconjugation of B^{III} and Cr^{III} co-doped $ZnGa_2O_4$ persistent luminescent nanoparticles for dual-targeted cancer bioimaging

Huai-Xin Zhao,[a] Cheng-Xiong Yang[a] and Xiu-Ping Yan*[ab]

[a] College of Chemistry, Research Center for Analytical Sciences, State Key Laboratory of Medicinal Chemical Biology (Nankai University), Tianjin Key Laboratory of Molecular Recognition and Biosensing, Nankai University, 94 Weijin Road, Tianjin 300071, China.

[b] Collaborative Innovation Center of Chemical Science and Engineering (Tianjin), Tianjin 300071, China.

Table of Contents

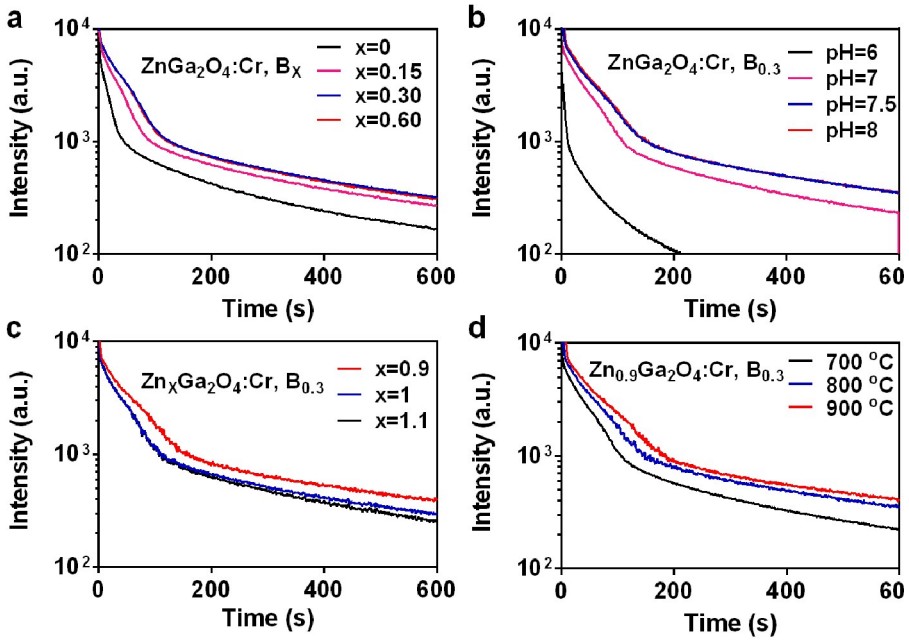

Fig. S1 The persistent luminescence decay curve of PLNP powder monitored at 694 nm after 5 min irradiation with a UV lamp: (a) Different doped content of boron; (b) Different pH for precipitation; (c) Different doped content of zinc; (d) Calcination temperature.

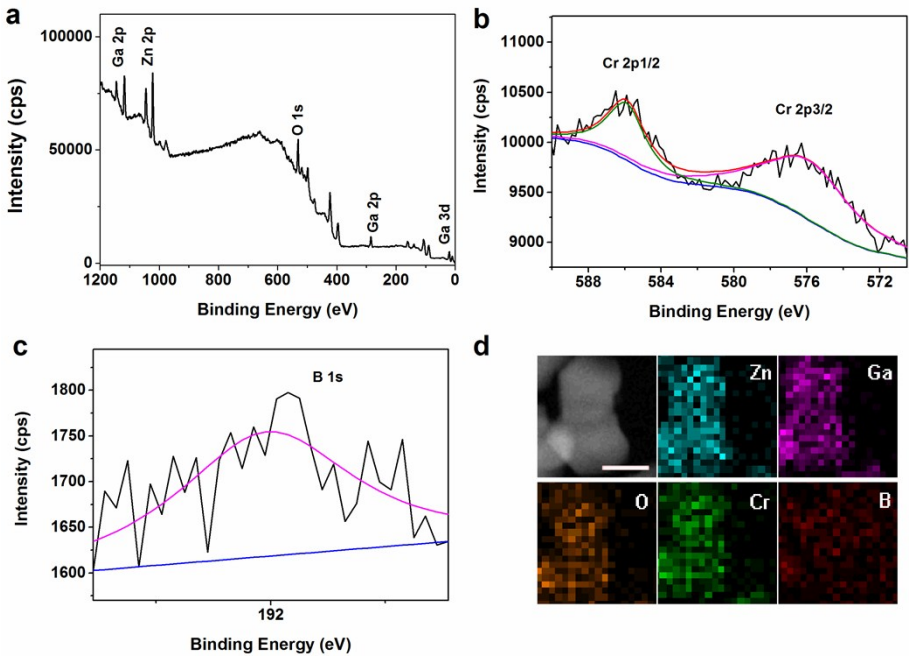

Fig. S2 (a) XPS survey scan of PLNP from 0-1200 eV. (b) High-resolution XPS spectrum of the Cr in PLNP. (c) High-resolution XPS spectrum of B 1s. (d) The large scale HAADF-STEM image and the corresponding elemental mapping of PLNP (the scale bar was 50 nm).

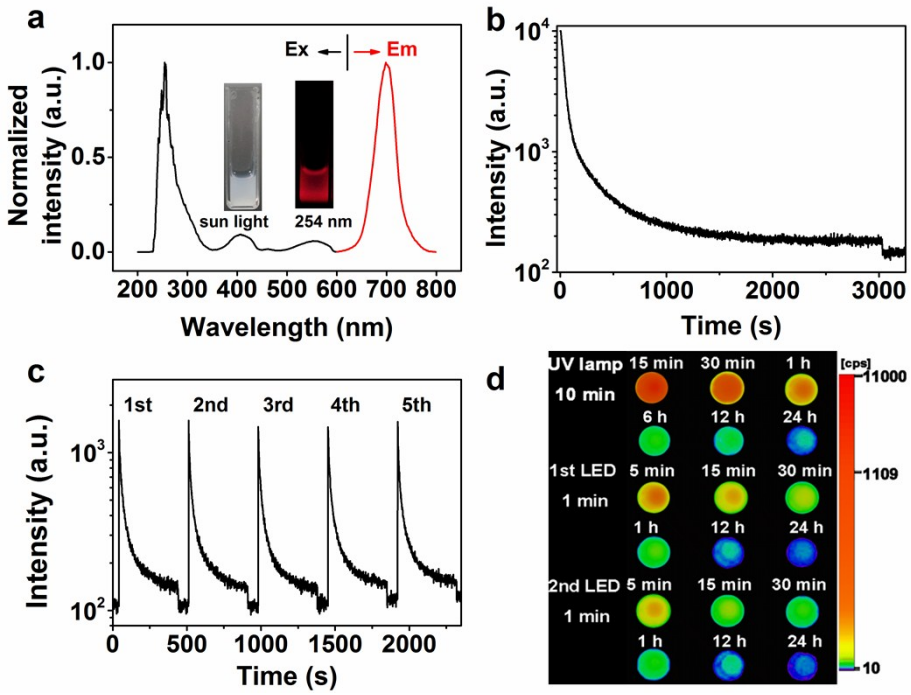

Fig. S3 Near-infrared persistent luminescence properties of the as-prepared PLNP dispersion (3 mg mL^{-1}): (a) Excitation and emission spectra; (b) NIR persistent luminescence decay curve excited with UV lamp for 10 min and monitored at 700 nm; (c) LED light-reactivated NIR persistent luminescence decay curves monitored at 700 nm after excitation with 650 nm LED for 1 min; (d) Persistent luminescence and re-activated persistent luminescence images recorded by CCD camera.

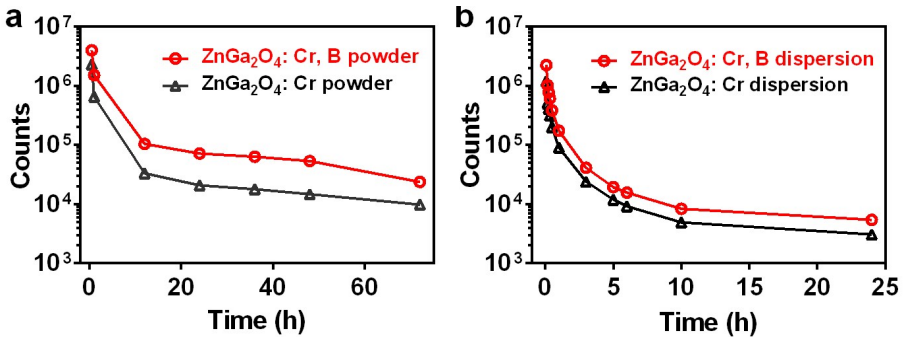

Fig. S4 NIR persistent luminescence decay curves of $ZnGa_2O_4$: Cr, B and $ZnGa_2O_4$: Cr powder (200 mg) and dispersion (3 mg mL^{-1}) recorded by CCD camera, respectively.

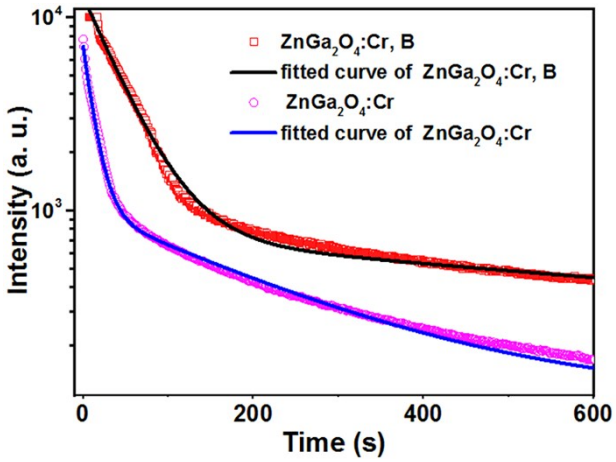

Fig. S5 The NIR persistent luminescence decay curves and the fitting curves of $ZnGa_2O_4$: Cr, B powder and $ZnGa_2O_4$: Cr powder.

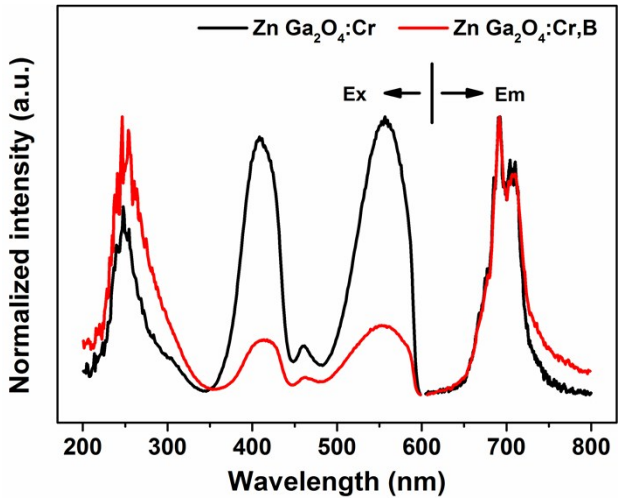

Fig. S6 Excitation and emission spectra of $ZnGa_2O_4$:Cr and $ZnGa_2O_4$:Cr, B powder.

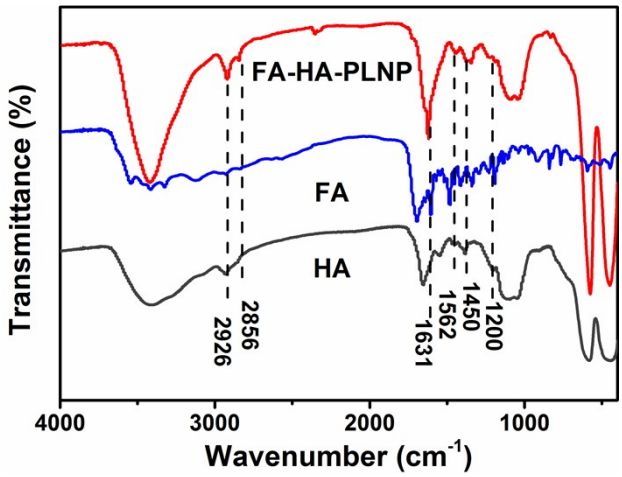

Fig. S7 FT-IR spectra of FA, HA and FA-HA-PLNP.

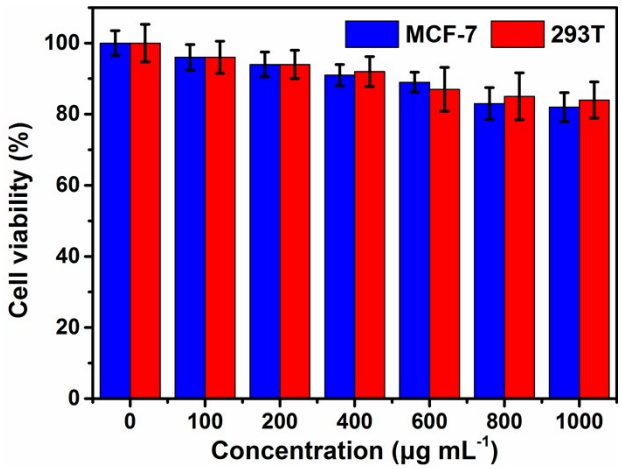

Fig. S8 In vitro cell viability of 293T cells and MCF-7 cells (incubation for 24 h, n=3).

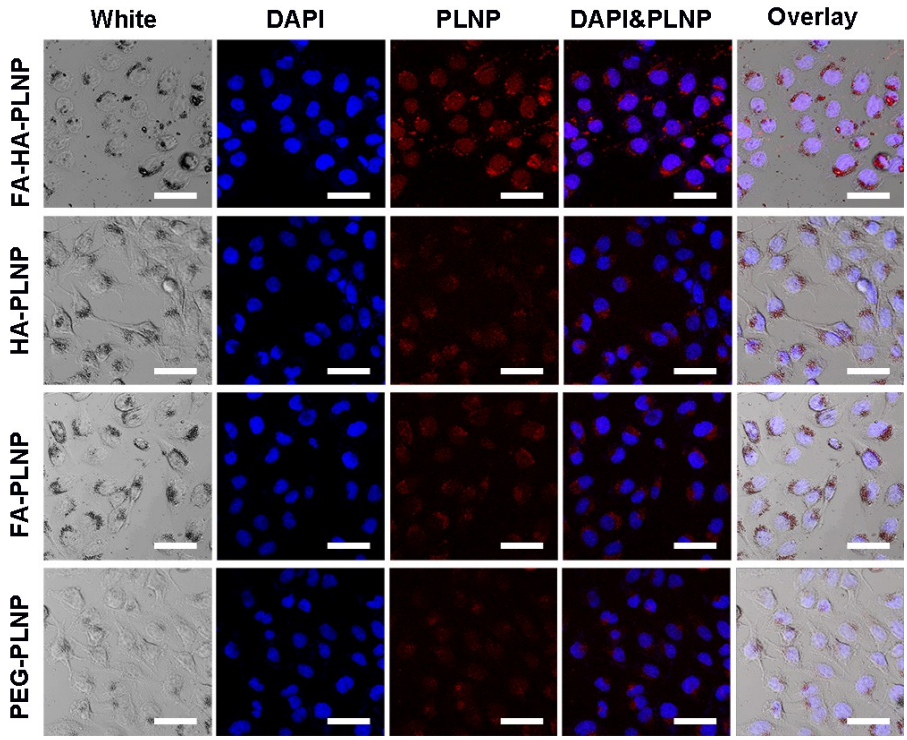

Fig. S9 Targeted *in vitro* fluorescence imaging of MCF-7 cell incubated with PEG-PLNP, FA-PLNP, HA-PLNP or FA-HA-PLNP. Scale bar is 50 μm.

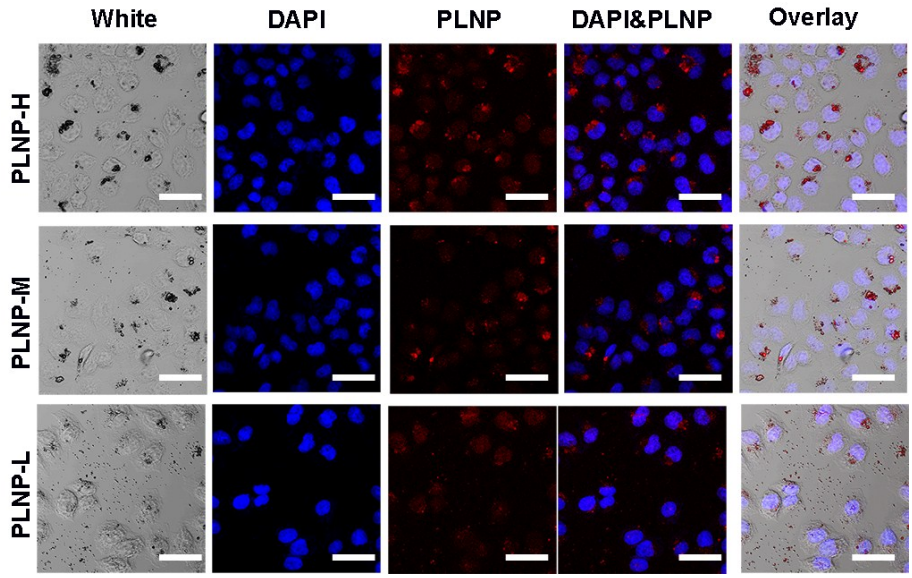

Fig. S10 Targeted *in vitro* fluorescence imaging of MCF-7 cell incubated with different conjugation efficiencies of ligands from high to low denoted as PLNP-H, PLNP-M, PLNP-L, which were prepared with different ratios of PLNP, HA and FA, 30 mg:150 mg:0.3 mg; 30 mg:20 mg: 0.04 mg and 30 mg: 5 mg: 0.01 mg, respectively. The PLNP-H with higher conjugation efficiency shows a better intracellular uptake. Scale bar is 50 μm.

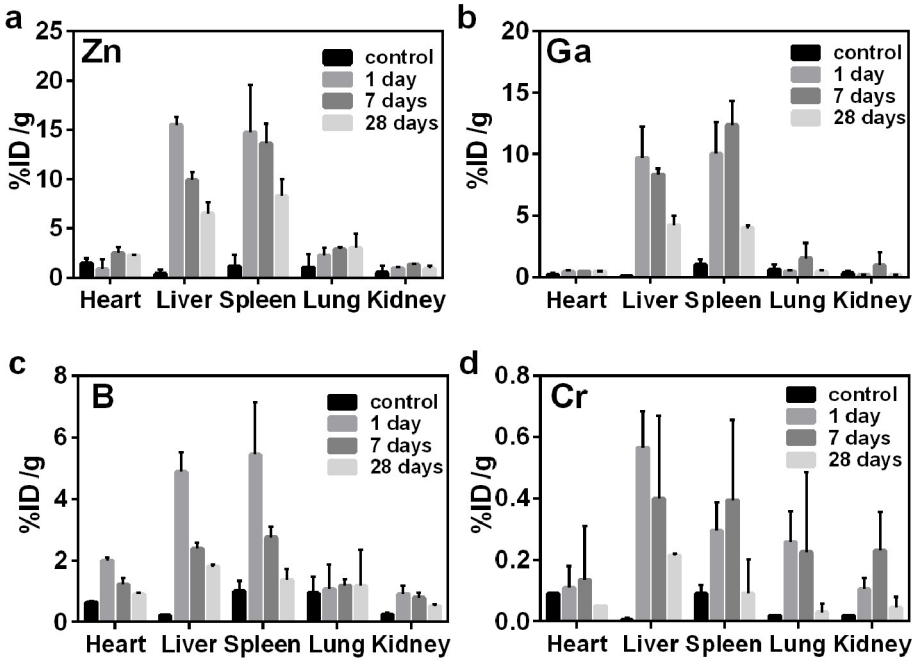

Fig. S11 Distribution of Zn (a), Ga (b), B (c) and Cr (d) in different organs of Kunming mice at different time (0, 1, 7, 28 days) as measured by ICP-MS after intravenous administration of the FA-HA-PLNP in PBS (250 mg kg^{-1}) (n=3). The unit is the percentage of injected dose per gram of tissue (%ID g^{-1}).

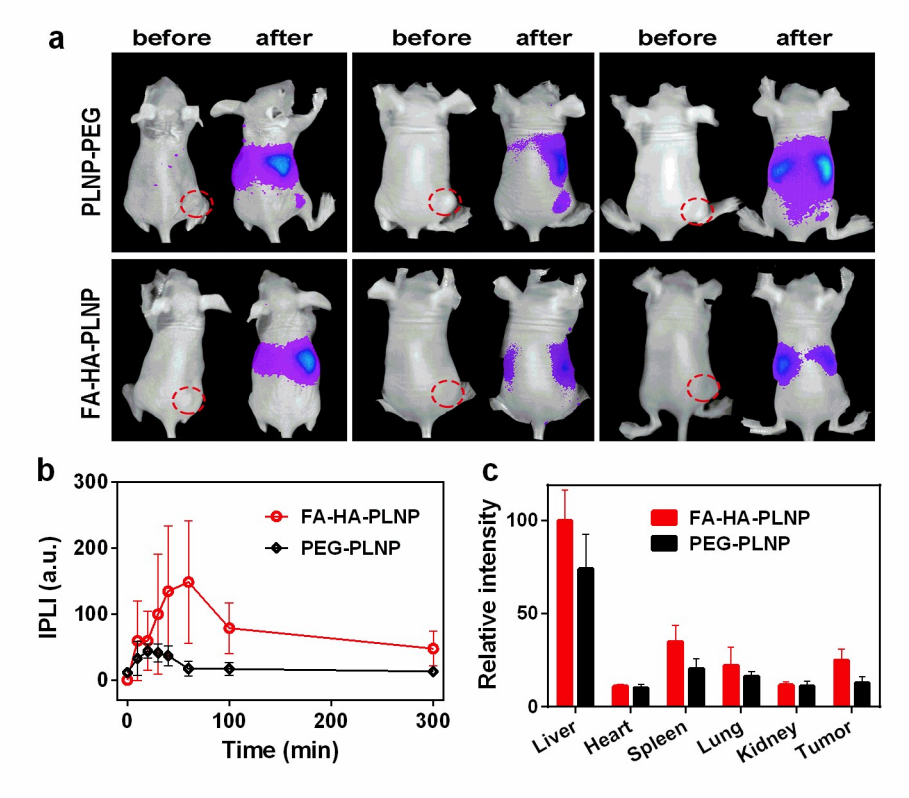

Fig. S12 (a) Persistent luminescent imaging of three tumour bearing mice before & after injection with PLNP-PEG or FA-HA-PLNP, respectively. (b) Increment of persistent luminescence intensity (IPLI) of tumour site pre-&post- injection of the nanoparticle. (c) Semi-quantification of PLNP in the isolated organs of treated tumour-bearing mice shown in (a).